

Robust and Imperceptible Dual Watermarking for Telemedicine Applications

Amit Kumar Singh · Basant Kumar · Mayank Dave · Anand Mohan

Published online: 30 September 2014
© Springer Science+Business Media New York 2014

Abstract In this paper, the effects of different error correction codes on the robustness and imperceptibility of discrete wavelet transform and singular value decomposition based dual watermarking scheme is investigated. Text and image watermarks are embedded into cover radiological image for their potential application in secure and compact medical data transmission. Four different error correcting codes such as Hamming, the Bose, Ray-Chaudhuri, Hocquenghem (BCH), the Reed–Solomon and hybrid error correcting (BCH and repetition code) codes are considered for encoding of text watermark in order to achieve additional robustness for sensitive text data such as patient identification code. Performance of the proposed algorithm is evaluated against number of signal processing attacks by varying the strength of watermarking and covers image modalities. The experimental results demonstrate that this algorithm provides better robustness without affecting the quality of watermarked image. This algorithm combines the advantages and removes the disadvantages of the two transform techniques. Out of the three error correcting codes tested, it has been found that Reed–Solomon shows the best performance. Further, a hybrid model of two of the error correcting codes (BCH and repetition code) is concatenated and implemented. It is found that the hybrid code achieves better results in terms of robustness. This paper provides a detailed analysis of the obtained experimental results.

A. K. Singh (✉)
Department of CSE and ICT, Jaypee University of Information Technology, Solan,
Himachal Pradesh, India
e-mail: amts.juit@gmail.com

B. Kumar
Department of Electronics & Communication Engineering, Motilal Nehru
National Institute of Technology, Allahabad, India

M. Dave
Department of Computer Engineering, NIT Kurukshetra, Kurukshetra, India

A. Mohan
Department of Electronics Engineering, IIT (BHU), Varanasi, Uttar Pradesh, India

Keywords Image watermarking · Steganography · Discrete wavelet transforms · Singular value decomposition · Error correcting codes

1 Introduction

Recently, telemedicine has played an important role in establishing health care facilities in remote and rural areas with the use of advanced information and communication technologies. Secure transmission and storage of electronic patient record (EPR) data between two hospitals via open channel are crucial issues in this field. Digital imaging and communications in medicine (DICOM) is a basic criterion to communicate EPR data. A header is attached with the DICOM medical image files which contain important information about the patient, but it may be lost, attacked or attached with medical image file wrongly. Digital watermarking is a technique which provides a best solution to these important issues [1]. These watermarks are difficult to remove by unauthorized person and they are robust against known or accidental attacks. The image watermarking technique is divided into two domain method [2]: (1) Spatial domain methods [3,4] (least significant bit substitution, spread spectrum etc.) are simple, high capacity but are not robust against common signal processing attacks. (2) Transform domain methods (DFT, DWT, DCT, and SVD etc.) are more robust against common signal processing attacks but the computational complexity is higher than that of spatial domain methods. The major characteristics of digital watermark are robustness, security, capacity and imperceptibility, and computational complexity, which have been discussed in detail [5]. The method proposed in [6] embeds multiple watermarks and improves robustness by using quantized wavelet coefficients and BCH code. Also, the method proposed in [7,8] embeds multiple watermarks where, these proposed methods achieved the copyright protection and image authentication simultaneously.

Dhanalakshmi and Thaiyalnayaki [9] proposed a dual watermarking method based on DWT-SVD and chaos encryption. They have embedded secondary watermark into primary watermark and the resultant watermark has been encrypted. Now, the combined encrypted watermark has been embedded into the cover image. The method proposed in [10] is also embedding multiple watermarks in the cover image. In the embedding process, a sign is first embedded into logo image and then a signed logo is embedded into the cover image. Also, pseudo random generator based on the mathematical constant π has been developed and used at different stages in the method. Mahajan and Patil [11] have proposed a dual watermarking method based on DWT-SVD. In the watermark embedding process, first the secondary watermark is embedded into primary watermark then the combined watermark is embedded into the cover image. The Secondary watermark is easy to detect however, the primary watermark is harder against various attacks. Kumar et al. [12] have been proposed an algorithm for text watermark representing each character in binary format using ASCII codes. BCH code is used to enhance the bit error rate (BER) performance of the extracted watermark.

Terzija et al. [13] have proposed a method for improving the efficiency and robustness of the image watermarks. Three different error correction codes, (15,7)-BCH, (7,4)-Hamming Code and (15-7)-Reed–Solomon code, are applied to the ASCII representation of the text Universitaet Duisburg which is being used as watermark. For embedding, the original image is first decomposed up to second level using the discrete wavelet transform with the pyramidal structure and watermark is added to the largest coefficients in all bands of details which represent the high and middle frequencies of the image. The Reed–Solomon code shows the best results due to its excellent ability to correct errors. However, the limitation of the proposed technique is that, it is unable to correct the error rates greater than 20 %. Lai and

Tsai [14] proposed a hybrid image-watermarking scheme based on DWT and SVD. After the first level decomposition of the cover image by Haar wavelet, SVD is applied to selected sub-band only. Now, dividing the watermark image into two parts, singular values in high-low (HL) and low-high (LH) sub-band are modified with half of the watermark image and then SVD is applied over them. The watermark extraction is just reversing the embedding process. With SVD, small modification of singular values does not affect the visual recognition of the cover image, which improves the robustness and transparency of the method. However, computational cost is high and the proposed method uses SVD transform technique that requires extra storage.

Singh et al. [15] proposed a DWT-SVD-ECCs based watermarking method where they combined Lai and Terzija method and the effects of the Hamming, the BCH, and the Reed–Solomon error correcting codes on the robustness and the image quality are investigated. Out of these error correction codes, Reed–Solomon has been shown the best performance. In this paper, we are using the hybrid error correcting code to improve the performance of the method. We are also using Lai method to embed the image watermark and Terzija method to embed text watermark. However, these watermarking methods embed only one watermark either text or image. We have combined these two concepts and embedded two watermarks (text and image) instead of single watermark into same multimedia object. The embedding dual watermarks in same multimedia object have significant advantages on various applications such as such as telemedicine and tele-diagnosis. There are three methods for dual watermark embedding, we can embed two watermarks either one after another [16, 17] or simultaneously [18].

In the proposed method, we are embedding two watermarks (text and image) simultaneously. The embedding image watermarks method is based on DWT and SVD. However, different ECCs (Hamming, BCH, Reed–Solomon code and hybrid code) are applied to the ASCII representation of text and embedded in the second level sub-band of the cover image, being used as text watermark. The algorithm correctly extracts the embedded watermarks without error and is robust against number of signal processing attacks without much degradation of the image quality of the watermarked image. The influences of the ECCs are compared and evaluated.

2 Discrete Wavelet Transforms (DWT)

The DWT is a filters based system, which decomposes an image into a set of four non-overlapping multi-resolution [19] sub bands denoted as LL (Approximation sub band), LH (Horizontal sub-band), HL (Vertical sub-band) and HH (Diagonal sub-band), where LH, HL, and HH subband represent the finest scale wavelet coefficients and LL subband stands for the coarse-level coefficients. The process can be repeated to obtain multiple scale wavelet decomposition, which is shown in Fig. 1.

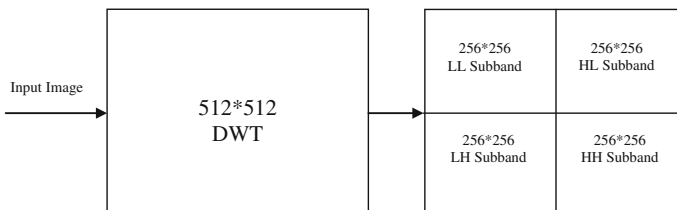


Fig. 1 First level of decomposition of the input image

3 Singular Value Decomposition (SVD)

The singular value decomposition of a rectangular matrix A is as follows [20]:

$$A = USV^T \quad (1)$$

where A is an $M \times N$ matrix, U and V are the orthonormal matrices. S is a diagonal matrix which consists of singular values of A . The singular values $s_1 \geq s_2 \geq \dots \geq s_n \geq 0$ appear in the descending order along with the main diagonal of S . However, these singular values have been obtained by taking the square root of the eigenvalues of AA^T and $A^T A$. These singular values are unique, however the matrices U and V are not unique. The SVD has two main properties from the viewpoint of image processing applications are: (1) the singular values of an image have very good stability, when a small perturbation is added to an image, its singular values do not change significantly, and (2) singular values represent the intrinsic algebraic image properties.

4 Performance Measures

The performance of the watermarking algorithm can be evaluated on the basis of its robustness and imperceptibility. A larger peak signal to noise ratio (*PSNR*) indicates that the watermarked image more closely resembles the original image meaning that the watermark is more imperceptible. Generally, watermarked image with *PSNR* value greater than 28 is acceptable [4]. *PSNR* is defined as

$$PSNR = 10 \log \frac{(255)^2}{MSE} \quad (2)$$

where the mean square error (*MSE*) is defined as

$$MSE = \frac{1}{X \times Y} \sum_{i=1}^X \sum_{j=1}^Y (I_{ij} - W_{ij})^2 \quad (3)$$

where I_{ij} is a pixel of the original image of size $X \times Y$ and W_{ij} is a pixel of the watermarked image of size $X \times Y$. The robustness of the algorithm is determined in term of correlation factor. The similarity and differences between original watermark and extracted watermark is measured by the normalized correlation (*NC*). Its value is generally 0 to 1. Ideally it should be 1 but the value 0.7 is acceptable [4].

$$NC = \frac{\sum_{i=1}^X \sum_{j=1}^Y (W_{originalij} \times W_{recoveredij})}{\sum_{i=1}^X \sum_{j=1}^Y W_{originalij}^2} \quad (4)$$

where $W_{originalij}$ is a pixel of the original watermark of size $X \times Y$ and $W_{recoveredij}$ is a pixel of the recovered watermark of size $X \times Y$. The bit error rate (*BER*) is defined as ratio between number of incorrectly decoded bits and total number of bits. It is suitable for random binary sequence watermark. Ideally it should be zero.

$$BER = (Number\ of\ incorrectly\ decoded\ bits) / (Total\ number\ of\ bits) \quad (5)$$

5 Error Correction Codes

The watermarking channel is characterized by very high error rates. To correct these errors we use different error correction schemes. Four families of error correcting schemes are used in our study to enhance the robustness of the watermark—repetition codes [21], Hamming codes,

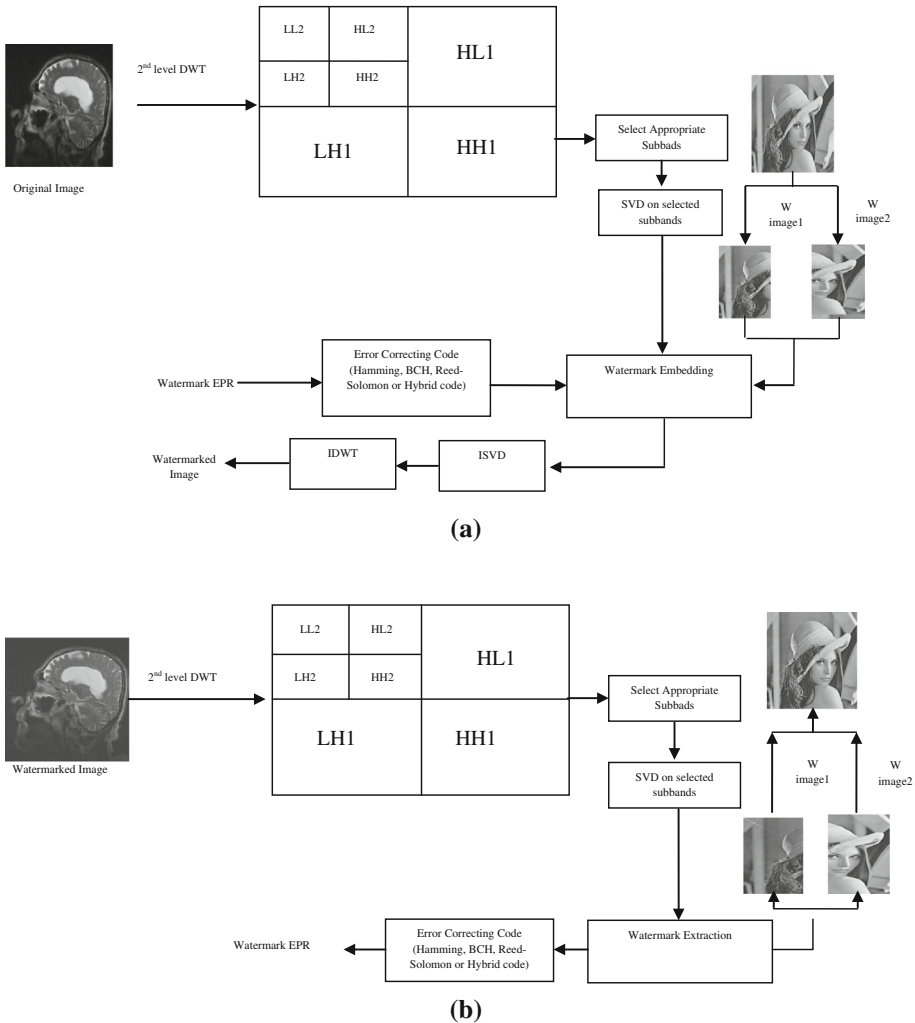


Fig. 2 a Watermark embedding algorithm, b Watermark extraction algorithm

BCH codes and Reed–Solomon codes [22]. In the error correcting process, the sender adds redundant bits to the original message which is used for error detection or error correction on the receiver side. In this process, we need to know the exact number of bits that are corrupted and their location in the message. By considering these ECCs we try to find trade-off between the number of bits to be embedded and the number of bit error can be corrected. However, if we employ a hybrid model where two of these error correcting codes are concatenated, robustness performance is expected to further improve.

6 Proposed Algorithm

The watermark embedding and extraction method is as shown in Fig. 2a, b, respectively. In the embedding process, the cover image is decomposed at second level DWT. The image

watermark is embedded into intermediate frequency subbands (HL and LH) of the first level DWT and the text watermark is embedded into higher coefficients subband (HH2) of the second level DWT. The proposed algorithm has two parts: (1) embedding and (2) extraction for image watermark (watermark 1) and embedding and extraction for text watermark (watermark 2), as given below:

Embedding algorithm for image watermark

start:

STEP 1: Variable Declaration

Medical Image(MRI): cover image

Lena: watermark image

C_w : read the cover image

W_w : read the watermark image

α : scale factor

DWT and SVD: Transform Domain Techniques

Wavelet filters: Haar

LL_c, HL_c, LH_c and HH_c : First level DWT coefficients for cover image

$LL_{c1}, HL_{c1}, LH_{c1}$ and HH_{c1} : Second level DWT coefficients for cover image

S_{c1} : diagonal matrix for HL_c

S_{c2} : diagonal matrix for LH_c

U_{c1} and V_{c1}^T : orthonormal matrices for HL_c

U_{c2} and V_{c2}^T : orthonormal matrices for LH_c

α : scale factor

W_{ck}^k : modified value of S_{ck}

U_{cw}^k and V_{cw}^{kT} : orthonormal matrices for W_w^k

S_{cw}^k : diagonal matrix for W_w^k

W_{kmodi} : Modified DWT coefficient

W_d : Watermarked Image

STEP 2: Read the Images

$M_w \leftarrow$ MRI.bmp (Cover image of size 512*512)

$L_w \leftarrow$ Lena.bmp (Watermark image of size 256*256)

STEP 3: Perform DWT on Cover image

Apply second level DWT on cover image and first level DWT on Watermark image

$[LL_c, HL_c, LH_c$ and $HH_c] \leftarrow$ DWT (M_w , wavelet filter);

$[LL_{c1}, HL_{c1}, LH_{c1}$ and $HH_{c1}] \leftarrow$ DWT (LL_c , wavelet filter);

STEP 4: Choice of subbands in Cover and apply SVD on the selected subbands

//Choose subband HL_c and LH_c from cover image

if (SVD on HL_c)**then**

$U_{c1} S_{c1} V_{c1}^T \leftarrow$ SVD (HL_c)

endif;

if (SVD on LH_c) **then**

$U_{c2} S_{c2} V_{c2}^T \leftarrow$ SVD (LH_c)

endif;

STEP 5: Watermark Embedding

//Divide the watermark into two parts $W = W1+W2$, modify the singular values in HL_{c1} and LH_{c1} subbands with half of the watermark image

for $\alpha \leftarrow 0.01: 0.1$

$S_{ck} + \alpha W_k = W_w^k; k=1,2$

end;

STEP 6: Compute the singular values for W_w^k and obtain the modified DWT coefficients

if (SVD on W_w^k)**then**

$[U_{cw}^k S_{cw}^k V_{cw}^{kT} \leftarrow$ SVD(W_w^k)

endif;

//modified DWT coefficient

$W_{kmodi} \leftarrow U_{ck} S_{cw}^k V_{ck}^T$

Step 7: Obtain the Watermarked Image W_d

//Apply inverseDWT to LL_c, HL_c, LH_c and HH_c using two sets of modified DWT coefficients and two sets of unmodified DWT coefficients.

$W_d \leftarrow$ inverse DWT(LL_c, HL_c, LH_c and HH_c , wavelet filter);

end;

Extraction Algorithm for image watermark**start:****STEP 1: Variable Declaration** α : scale factor LL_c, HL_c, LH_c and HH_c : subbands for watermarked image S_{cw1} : orthonormal matrices for HL_c S_{cw2} : orthonormal matrices for LH_c U_{cw1} and V_{cw1}^T : orthonormal matrices for HL_c U_{cw2} and V_{cw2}^T : orthonormal matrices for LH_c DW : modified singular value of selected subbands of cover image Wk : extracted watermark $k=1$ and 2 **STEP 2: Perform DWT on Watermarked image (possibly distorted)** $[LL_c, HL_c, LH_c$ and $HH_c, \text{wavelet filter}] \leftarrow \text{DWT}(W_d, \text{wavelet filter});$ **STEP 3: Compute the singular values for HL_c and LH_c subbands**//Apply SVD to HL_c, LH_c subbands**if** (SVD on HL_c)**then** $U_{cw1}S_{cw1}V_{cw1}^T \leftarrow \text{SVD}(HL_c)$ **endif;****if** (SVD on LH_c) **then** $U_{cw2}S_{cw2}V_{cw2}^T \leftarrow \text{SVD}(LH_c)$ **endif;****STEP 4: Compute DW**

//modify the singular value of cover image

 $DW \leftarrow U_{cw}^k S_{cwk} V_{cw}^{kT}; k=1,2$ **STEP 5: Extract the half of the watermark image from each subband and combined** $Wk = \frac{DW - S_{ck}}{\alpha}; k=1,2$ **end:****Embedding Algorithm for Text Watermark****start:****STEP 1: Variable Declaration**

Medical Image(MRI): cover image

Lena: watermark image

 C_w : read the cover image W_w : read the watermark image α : scale factor

DWT : discrete wavelet transforms

Wavelet filters: Haar

 LL_c, HL_c, LH_c and HH_c : First level DWT coefficients for cover image $LL_{c1}, HL_{c1}, LH_{c1}$ and HH_{c1} : Second level DWT coefficients for cover image**STEP 2: Read the Images** $M_w \leftarrow \text{MRI.bmp}$ (Cover image of size 512*512)**STEP 3: Perform DWT on Cover image**

//Apply second level DWT on cover image

 $[LL_c, HL_c, LH_c$ and $HH_c] \leftarrow \text{DWT}(M_w, \text{wavelet filter});$ $[LL_{c1}, HL_{c1}, LH_{c1}$ and $HH_{c1}] \leftarrow \text{DWT}(LL_c, \text{wavelet filter});$ **STEP 4: Convert Watermarking text to Binary bits**

// converting text watermark (JUIT) into binary bits

 $W_{txt} \leftarrow \text{binary}(\text{Amit_BXPBS4951D_MR19});$ **STEP 6: Perform error correcting codes to the watermarking bits just obtained to get the final watermarking bits.**//Apply the Hamming, the BCH, the Reed-Solomon or the hybrid error correcting code to the watermark bits W_b . $W_b \leftarrow \text{error correcting code}(\text{watermark bits})$ **STEP 5: Replace '(0,1)' by '(-1,1)' in the watermarking bits**// bit stream is transformed into a sequence $w(1) w(2) \dots w(L)$ by replacing the 0 by -1 and 1 by 1, L is the length of string

```

-1 ← 0 and 1 ← 1;
STEP 7: Embedding the text watermark
// text watermark is embeds into  $HH_{c1}$  subband
for  $\alpha \leftarrow 0.01:0.1$ 
 $f'(x,y) = f(x,y)(1+\alpha \times Wb)$ ;  $f(x,y)$  and  $f'(x,y)$  is DWT coefficients before and after embedding process
end;
STEP 8: Obtain the Watermarked Image  $W_d$ 
//Apply Inverse DWT to  $LL_c, HL_c, LH_c$  and  $HH_c$  with modified and unmodified DWT coefficients
 $W_d \leftarrow \text{inverse DWT}(LL_c, HL_c, LH_c \text{ and } HH_c, \text{wavelet filter})$ ;
end;

```

Extraction Algorithm for Text Watermark

In the watermark extraction procedure, both the received image and the original image are decomposed into the two levels. It is assumed that the original image is available for extraction process

```

start:
STEP 1: Variable Declaration
Medical Image(MRI): cover image
Lena: watermark image
C_w: read the cover image
W_w: read the watermark image
 $\alpha$ : scale factor
DWT: discrete wavelet transforms
Wavelet filters: Haar
 $LL_c, HL_c, LH_c$  and  $HH_c$ : First level DWT coefficients for cover image
 $LL_{c1}, HL_{c1}, LH_{c1}$  and  $HH_{c1}$ : Second level DWT coefficients for cover image
start:
STEP 2: Perform DWT on Watermarked image (possibly distorted)
// original image is also available for extraction process
 $[LL_c, HL_c, LH_c \text{ and } HH_c, \text{wavelet filter}] \leftarrow \text{DWT}(W_d, \text{wavelet filter})$ ;
STEP 3: Watermark extraction
 $W_r b = \frac{(f_r'(x,y) - f(x,y))}{\alpha f(x,y)}$ ;  $f_r'(x,y)$  are the DWT coefficients of the received image.
//finally extracted watermark taken as sign(either positive or negative)
 $W_e b \leftarrow \text{positive or negative sign}(W_r b)$ ;
STEP 4: Perform error correcting codes to  $W_e b$ 
// also modify the watermarking bits by replacing '(-1,1)' by '(0,1)' to get the final watermark.
 $W_f b \leftarrow \text{error correcting code}(W_e b)$ 
STEP 5: Convert the watermark bits into text to get the original watermark
Original text ← convert(watermark bits)
end:

```

7 Experimental Results and Discussion

We have described the performance of combined ECCs-DWT-SVD watermarking algorithm.

The gray-level medical images of size 512×512 [23] as cover image. The Lena image as image watermark and patient's identity/reference "Amit_BXBPS4951D_MR19" as text watermarks. The image watermark embedding method is based on DWT and SVD. However, the text watermark embedding method is based on different ECCs. The resulting bits are embedded in five different ways: without ECCs and coded by Hamming, BCH, Reed-Solomon and the hybrid code.

Without coded version we implement 140 bits according to 20 characters whereas each character uses only seven-bit ASCII instead of eight-bit ASCII value. The Hamming coded watermark has an amount of 245 bits. However, the encoded watermark length for BCH and Reed-Solomon is 300 bits. With repetition encoding, repeating each original signal of a watermark N times in a block section, named block section (N, 1). Here, we are using $N = 3$. We implemented proposed algorithm in MATLAB. The performance of the proposed algorithm is evaluated in terms of imperceptibility and robustness against various signal

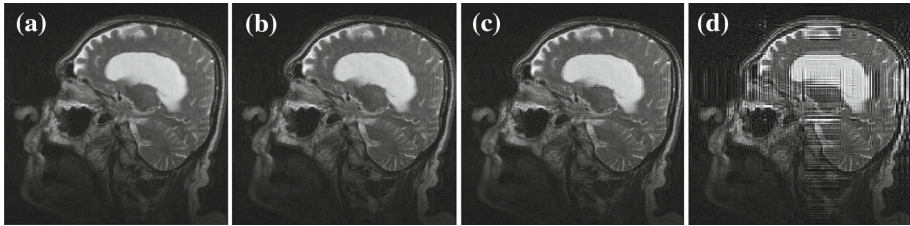


Fig. 3 Original and watermarked MRI images **a** original image and watermarked images with gain factor; **b** 0.01; **c** 0.05 and **d** 0.5

Patient’s name _Patient’s identity_Image code: Amit_BXBPS4951D_MR19

Fig. 4 EPR data as watermark

Table 1 Hamming code performance at different gain

Gain (α)	1st level DWT decomposition					1st level DWT decomposition					2nd level DWT decomposition				
	PSNR at various value of text (bits)					NC value for image watermark					BER value for text watermark				
	28	56	84	112	140	28	56	84	112	140	28	56	84	112	140
0.01	40.93	39.22	38.34	37.72	37.22	0.8761	0.9043	0.9067	0.8921	0.8739	0	0	0	0	0
0.03	39.16	37.95	37.27	36.78	36.38	0.9890	0.9920	0.9927	0.9911	0.9881	0	0	0	0	0
0.05	35.89	35.28	34.89	34.61	34.36	0.9933	0.9948	0.9957	0.9958	0.9951	0	0	0	0	0
0.07	33.07	32.74	32.52	32.35	32.21	0.9923	0.9933	0.9937	0.9940	0.9938	0	0	0	0	0
0.09	30.82	30.61	30.48	30.37	30.28	0.9928	0.9933	0.9936	0.9939	0.9938	0	0	0	0	0
0.1	29.85	29.69	29.58	29.49	29.58	0.9929	0.9933	0.9934	0.9936	0.9934	0	0	0	0	0

processing attacks. The PSNR is used to measure the quality of the watermarked image. However, robustness of the extracted watermark is measured by NC and BER. Also, the influences of the ECCs are compared and evaluated. Figure 3 shows the cover CT scan image and watermarked images obtained at different gain factors. Figure 4 shows the EPR data using as a text watermark. In the experiments, we use the gain factor (α) as 0.01 to 0.1 and the value of PSNR, NC and BER are illustrated in Tables 1, 2, 3, 4, 5, and 6. However, Table 7 shows the superior performance of hybrid code over the other three error correcting code. Without any noise attack, highest PSNR obtained with error correcting codes (140 text bits) is 37.22dB at $\alpha = 0.01$ whereas NC = 1 and BER = 0 at all chosen gain factors. We found that larger the gain factor, stronger the robustness and smaller the gain factor, better the image quality. In Table 1, hamming code performance up to 140 text bit has been evaluated without any noise attack. The maximum NC value is 0.9951 at $\alpha = 0.05$ against 140 bits (maximum bits). In Table 2, Hamming code performance of the proposed algorithm have been evaluated at $\alpha = 0.05$ against different signal processing attacks. The highest NC value have been obtained against JPEG compression (quality factor = 100). It is 0.9949. However, the lowest NC is 0.3011 against salt and pepper noise with density 0.1. The highest BER have been found 8.5714 against Gaussian noise. Without Hamming code it was 10.

In Table 3, BCH code performance up to 140 bit has been evaluated without any noise attack. The maximum PSNR value is 36.85 at $\alpha = 0.05$. However, the maximum NC value is

Table 2 Hamming code performance at gain = 0.05 against different attacks

Attacks	With Hamming coding		Without Hamming coding	
	Image watermark (NC value)	Text watermark (BER Value)	Image watermark (NC value)	Text watermark (BER value)
JPEG compression (QF-100)	0.9950	0	0.9955	0
JPEG compression (QF-60)	0.9325	0	0.9528	0
JPEG compression (QF-20)	0.9653	0	0.9582	0
Sharpening mask with threshold=0.1, 0.3, 0.5, 0.7 and 0.9	0.6073, 0.6257, 0.6390, 0.6486 and 0.6556	0	0.6338, 0.6507, 0.6630, 0.6711 and 0.6769	0
Median filtering [2 2] and [3 3]	0.9116 and 0.8885	0	0.9077 and 0.8856	0.7143 and 0
Scaling factor 2	0.7075	0	0.7172	0.7143
Scaling factor 2.5	0.6500	1.0126	0.659	1.4286
Gaussian LPF with standard deviation = 0.6	0.8780	0	0.8672	0
Gaussian noise with mean = 0, Var = 0.001	0.7012	0	0.7101	0
Gaussian noise with mean = 0, Var = 0.05	0.3150	8.5714	0.3264	10
Salt & pepper noise with (Density = 0.001)	0.7553	0	0.7880	0
Salt & pepper noise with (Density = 0.1)	0.3011	0	0.3083	0.7143
Histogram equalization	0.5880	1.4286	0.5931	2.1429
Cropping attack	0.7451	4.5714	0.7173	5

0.9940 at $\alpha = 0.05$ against 140 bits (maximum text bits). In Table 4, BCH code performance of the proposed algorithm have been evaluated at $\alpha = 0.05$ against different signal processing attacks. The highest NC value have been obtained against JPEG compression (quality factor =100). It is 0.9942. However, the lowest NC is 0.3086 against salt and pepper noise with density 0.1. The highest BER have been found 6.284 against Gaussian noise. Without BCH code it was 10.

In Table 5, Reed–Solomon code performance up to 140 bit has been evaluated without any noise attack. The maximum PSNR value is 36.85 at $\alpha = 0.05$. However, the maximum NC value is 0.9943 at $\alpha = 0.05$ against 140 bits (maximum text bits). In Table 6, Reed–Solomon code performance of the proposed algorithm have been evaluated at $\alpha = 0.05$ against different signal processing attacks. The highest NC value have been obtained against JPEG compression (quality factor =100). It is 0.9939. However, the lowest NC is 0.3085

Table 3 BCH code performance at different gain

Gain (α)	1st level DWT decomposition					1st level DWT decomposition					2nd level DWT decomposition				
	PSNR at different number of bits					NC value for image watermark at different number of bits					BER value for text watermark at different number of bits				
	28	56	84	112	140	28	56	84	112	140	28	56	84	112	140
0.01	40.41	38.79	37.88	37.29	36.85	0.8759	0.893	0.8887	0.8784	0.8472	0	0	0	0	0
0.03	38.81	37.62	36.91	36.44	36.07	0.9888	0.9907	0.9902	0.9882	0.9833	0	0	0	0	0
0.05	35.72	35.09	34.69	34.39	34.16	0.9936	0.9950	0.9955	0.9957	0.9943	0	0	0	0	0
0.07	32.98	32.64	32.39	32.23	31.34	0.9926	0.9935	0.9939	0.9940	0.9938	0	0	0	0	0
0.09	30.76	30.55	30.40	30.29	29.70	0.9928	0.9934	0.9940	0.9939	0.9938	0	0	0	0	0
0.1	29.80	29.64	29.52	30.09	29.35	0.9930	0.9934	0.9936	0.9936	0.9933	0	0	0	0	0

Table 4 BCH code performance at gain = 0.05 against different attacks

Attacks	With BCH coding		Without BCH coding	
	NC value for image watermark	BER Value for Text Watermark	NC value for image watermark	BER value for text watermark
JPEG compression (QF-100)	0.9942	0	0.9955	0
JPEG compression (QF-60)	0.9234	0	0.9528	0
JPEG compression (QF-20)	0.9723	0	0.9676	0
Sharpening mask with threshold = 0.1,0.3,0.5,0.7 and 0.9	0.5986, 0.6161, 0.6293, 0.6388 and 0.6457	0	0.6338, 0.6507, 0.6630, 0.6711 and 0.6769	0
Median filtering [2 2] and [3 3]	0.9144 and 0.8896	0	0.9077, 0.8856	0.7143 and 0
Scaling Factor 2	0.699	0	0.7172	0.7143
Scaling Factor 2.5	0.646	0.7112	0.659	1.4286
Gaussian LPF with standard deviation = 0.6	0.8612	0	0.8672	0
Gaussian noise with mean = 0, Var -0.001	0.7063	0	0.7121	0
Gaussian noise with mean = 0, Var -0.05	0.3284	6.2843	0.3264	10
Salt & pepper noise with (Density = 0.001)	0.7825	0	0.7880	0
Salt & pepper noise with (Density = 0.1)	0.3086	0	0.3083	0.7143
Histogram equalization	0.585	0.7143	0.5931	2.1429
Cropping attack	0.7449	3.5714	0.7173	5

Table 5 Reed–Solomon code performance at different gain

Gain (α)	1st level DWT decomposition					1st level DWT decomposition					2nd level DWT decomposition				
	PSNR at various value of text (bits)					NC value for image watermark at different number of bits					BER value for text watermark at different number of bits				
	28	56	84	112	140	28	56	84	112	140	28	56	84	112	140
0.01	40.41	38.79	37.88	37.29	36.85	0.8759	0.8989	0.8893	0.8607	0.8393	0	0	0	0	0
0.03	38.81	37.62	36.91	36.44	36.07	0.9884	0.9909	0.9905	0.9864	0.9827	0	0	0	0	0
0.05	35.72	35.09	34.69	34.39	34.16	0.9938	0.9954	0.9957	0.9950	0.9940	0	0	0	0	0
0.07	32.98	32.64	32.39	32.22	32.08	0.9927	0.9937	0.9940	0.9939	0.9934	0	0	0	0	0
0.09	30.76	30.55	30.40	30.29	30.20	0.9929	0.9934	0.9938	0.9938	0.9936	0	0	0	0	0
0.1	29.81	29.64	29.52	29.43	29.35	0.9930	0.9934	0.9935	0.9935	0.9934	0	0	0	0	0

Table 6 Reed–Solomon code performance at gain = 0.05 against different attacks

Attacks	With Reed–Solomon coding		Without Reed–Solomon coding	
	NC value for image watermark	BER value for text watermark	NC value for image watermark	BER value For text Watermark
JPEG compression (QF-100)	0.9939	0	0.9955	0
JPEG compression (QF-60)	0.9251	0	0.9528	0
JPEG compression (QF-20)	0.9665	0	0.9676	0
Sharpening mask with threshold = 0.1, 0.3, 0.5, 0.7 and 0.9	0.6028, 0.6207, 0.6338, 0.6431 and 0.6500	0	0.6338, 0.6507, 0.6630, 0.6711 and 0.6769	0
Median filtering [2 2] and [3 3]	0.9143 and 0.8896	0	0.9077, 0.8856	0.7143 and 0
Scaling Factor 2	0.7008	0	0.7172	0.7143
Scaling Factor 2.5	0.6444	0	0.659	1.4286
Gaussian LPF	0.8612	0	0.8872	0
Gaussian noise with mean = 0, Var -0.001	0.7011	0	0.7121	0
Gaussian Noise with mean = 0, Var -0.05	0.3141	6.1321	0.3264	10
Salt & pepper noise with (Density = 0.001)	0.7897	0	0.7880	0
Salt & pepper noise with (Density = 0.1)	0.3085	0	0.3083	0.7143
Histogram equalization	0.5833	0.6693	0.5931	2.1429
Cropping attack	0.7453	3.5022	0.7173	5

Table 7 Hybrid code performance at different gain

Gain (α)	1st level DWT decomposition			1st level DWT decomposition			2nd level DWT decomposition		
	PSNR at various value of text(bits)			NC value for image watermark at different number of bits			BER value for text watermark at different number of bits		
	28	84	140	28	84	140	28	84	140
0.01	37.87	35.75	35	0.8994	0.755	0.6921	0	0	0
0.05	34.68	33.54	33.07	0.9961	0.9876	0.9814	0	0	0
0.09	30.4	29.93	29.73	0.994	0.9922	0.9905	0	0	0
0.1	29.51	29.13	28.96	0.9936	0.9924	0.9912	0	0	0

against salt and pepper noise with density 0.1. The highest BER have been found 6.1321 against Gaussian noise. Without BCH code it was 10. With ECCs, NC is not acceptable in case of Gaussian noise and salt and pepper noise.

In Table 7, the hybrid error correcting code performance up to 140 bit has been evaluated without any noise attack. The maximum PSNR value is 35 at $\alpha = 0.01$. However, the maximum NC value is 0.9912 at $\alpha = 0.1$ against 140 bits (maximum text bits). Table 8 provides the performance comparison of hybrid error correcting with the other three error correcting codes. We are selecting only those attacks where the BER values are not zero. In this table, the maximum NC value with hybrid error correcting coding method has been obtained as 0.9481 against 0.7451, 0.7173 and 0.7451 obtained by hamming, BCH and Reed–Solomon error correcting code respectively. The maximum BER value has been obtained with hybrid method is 2.618 against Gaussian Noise (Mean = 0, Var = 0.05). However, BER value has been obtained with hamming, BCH and Reed–Solomon error correcting code are 8.5714, 10 and 8.5714 respectively. However, if we reduce the variance the noise, the image can be recovered without any error. Overall, the hybrid method is better than the other three error correcting codes methods.

Table 9 shows the effect of cover image, the hybrid error correcting code was tested for other medical images like CT scan, ultrasound and Barbara images at gain factor = 0.05. The highest NC value has been obtained with Barbara image. However, the highest PSNR value has been obtained with Ultrasound image. With all the images, BER value is zero. Also, we compare the performance of the hybrid error correcting code with Tripathi et al. [10] and Mahajan and Patil [11] against different kind of attacks. It can be seen that the results in Table 10, hybrid method gives better result than the other reported methods [10,11].

The graphical representation of the performance by the proposed method using hybrid error correcting code as shown in Figs. 5, 6, 7, and 8. Figures 5 and 6 shows the NC and BER values against different attacks respectively. In Fig. 5, the maximum NC value with hybrid code has been obtained as 0.9481 against the cropping attacks. However, the hamming, the BCH and the Reed–Solomon error correcting code have been obtained as 0.7451, 0.7173 and 0.7451 respectively. The minimum NC value with hybrid code has been obtained as 0.3232 against the salt & pepper noise with density = 0.1. However, the hamming, the BCH and the Reed–Solomon error correcting code have been obtained as 0.3011, 0.3083 and 0.3011 respectively. In Fig. 6, the maximum and minimum BER value with hybrid code has been obtained as 2.618 and zero against the Gaussian Noise (Mean = 0, Var = 0.05) and salt & pepper noise respectively. However, the maximum BER value with the hamming, the BCH and the Reed–Solomon error correcting code have been obtained as 8.5714, 10 and 8.5714 respectively.

Table 8 Performance comparison of different ECCs against signal processing attacks at gain = 0.05

Attacks	With Hamming coding		With BCH coding		With Reed–Solomon coding		With Hybrid coding	
	Image watermark (NC value)	Text watermark (BER value)	Image watermark (NC value)	Text watermark (BER value)	Image watermark (NC value)	Text watermark (BER value)	Image watermark (NC value)	Text watermark (BER value)
Scaling Factor 2.5	0.65	1.0126	0.659	1.4286	0.65	1.0126	0.692	0.3214
Gaussian noise with mean = 0, Var = 0.05	0.315	8.5714	0.3264	10	0.315	8.5714	0.3289	2.618
Salt & pepper noise (Density = 0.1)	0.3011	0	0.3083	0.7143	0.3011	0	0.3232	0
Histogram equalization	0.588	1.4286	0.5931	2.1429	0.588	1.4286	0.8187	0
Cropping attack	0.7451	4.5714	0.7173	5	0.7451	4.5714	0.9481	1.666

Table 9 Effect of cover images on the performance of proposed scheme using hybrid error correcting code at gain factor = 0.05

Image type	PSNR	NC value	BER value
MRI	28.45	0.9475	0
CT scan	29.21	0.9227	0
Ultrasound	32.45	0.9657	0
Barbara	25.87	0.9879	0

Table 10 Experimental results showing NC values against Tripathi et al. [10] and Mahajan and Patil [11]

Attacks	Tripathi et al. [10]	Mahajan and Patil [11]	Proposed hybrid method
Scaling (scaling factor = 0.5 and 1.5)	0.3137 and 0.7031	Not Tested	0.3922 and 0.831
Rotation (350 and 10°)	0.7478 and 0.7387	0.1413 rotation degree does not defined	0.8690 and 0.9110
JPEG compression (QF = 20)	0.9586	Not tested	0.9723
Salt & pepper noise	Not tested	-0.0013	0.3232
Cropping	Not tested	0.1411	0.9481

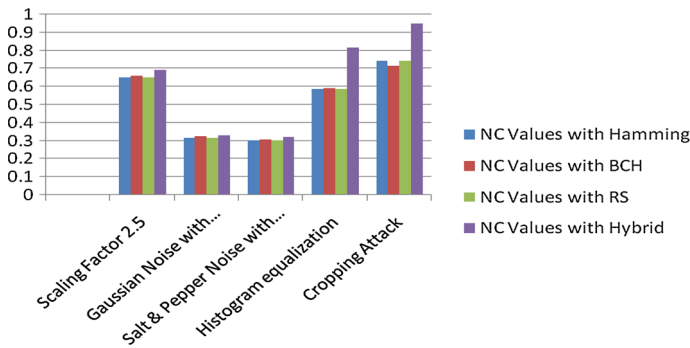


Fig. 5 NC values of the proposed method against different attacks at gain = 0.05 and text bit = 140

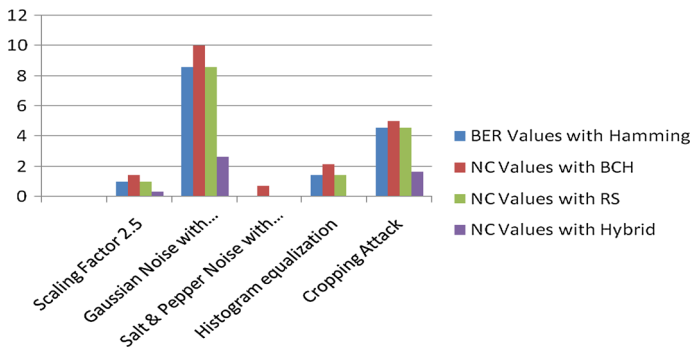


Fig. 6 BER values of the proposed method against different attacks at gain = 0.05 and text bit = 140

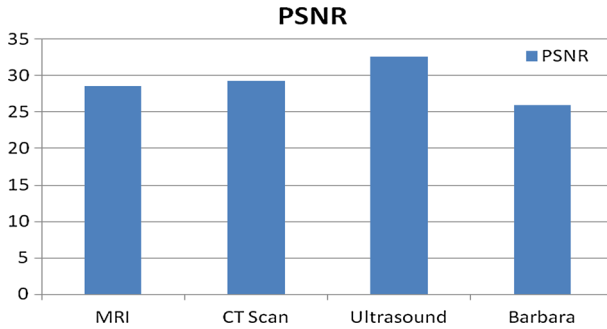


Fig. 7 PSNR values of the proposed method using hybrid error correcting code against different cover images at gain factor = 0.05

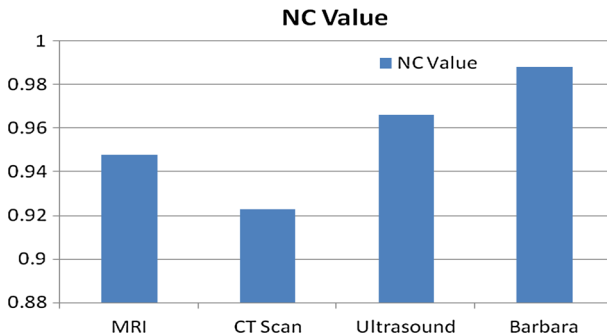


Fig. 8 BER values of the proposed method using hybrid error correcting code against different cover images at gain factor = 0.05

Figures 7 and 8 shows the performance of the proposed method with the hybrid error correcting code against the different cover images. In Fig. 7, the maximum PSNR value has been obtained 0.9879 with Ultrasound image. Its value is 32.45. However, the minimum PSNR value is 25.87 with the Barbara image. In Fig. 8, the highest NC value has been obtained 0.9879 with Barbara image. However, the minimum NC value is 0.9227 with the CT Scan image.

8 Conclusion and Future Directions

In this paper, we proposed a new approach for image and text watermarking. We have developed a robust non-blind dual watermarking algorithm based on DWT-SVD-ECCs. The DWT and SVD are novel techniques used for watermarking so their fusion makes a very attractive watermarking technique. Due to its excellent spatio-frequency localization properties, the DWT is very suitable to identify areas in the cover image where a watermark can be imperceptibly embedded. One of attractive mathematical properties of SVD is that slight variations of singular values do not affect the visual perception of the cover image, which motivates the watermark embedding procedure to achieve better imperceptibility and robustness. So, the proposed hybrid technique improves the robustness and imperceptibility as compared to DWT and SVD applied individually. In order to make the data error correctable, additional

bits in the form of ECC is required to be added in the original bits. However, if we want to further improve the error correction capability the length of the error correction code may be suitably increase. The main properties of the proposed work can be identified as follows: (1) Proposed algorithm combines the advantages and removes the disadvantages of these two most popular transforms namely DWT and SVD. (2) We have embedded two watermarks (text and image) instead of single watermark into same multimedia object which have great advantages on many applications such as telemedicine. (3) In the proposed method, we used the method which can embed two watermarks simultaneously which have fewer constraints than the other dual watermark embedding method. (4) Also, the first level decomposition has some advantages such as the watermark embedding is maximized, and the extracted watermarks are more textured with better visual quality.

We would like to further improve the performance, which will be reported in future communication.

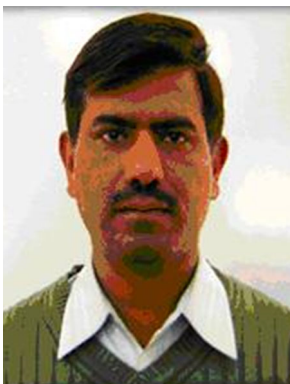
References

1. Mostafa, S. A. K. (2010). N El- sheimy, A S Tolba, F M Abdelkader, H M Elhindy, "Wavelet Packets-Based Blind Watermarking for Medical Image Management". *The Open Biomedical Engineering Journal*, 4, 93–98.
2. Peng, H., Wang, J., & Wang, W. (2010). Image watermarking method in multiwavelet domain based on support vector machines. *The Journal of Systems and Software*, 83, 1470–1477.
3. N Nikolaidis and I Pitas, "Digital Image Watermarking: An Overview", IEEE International Conference on Multimedia Computing and Systems, pp. 1–6, 1999.
4. Cox, I.J., & Miller, M., (2002). "The First 50 Years of Electronic Watermarking", *Journal on Applied Signal Processing*, pp. 126–132.
5. Singh, A.K., Dave, M. & Mohan, Anand (2014). "Wavelet Based Image Watermarking: Futuristic Concepts in Information Security", Proceedings of the National Academy of Sciences, India Section A: Physical Sciences, 2014, doi:10.1007/s40010-014-0140-x.
6. Giakoumaki, A., Pavlopoulos, S., & Koutsouris, D. (2006). Secure and Efficient Health Data Management through Multiple Watermarking on Medical Images. *Medical Biological Engineering & Computing*, 44, 619–631.
7. Chang, C.-C., Tai, W.-L., & Lin, C.-C. (2006). "A multipurpose wavelet-based image watermarking", Proc. International Conference on Innovative Computing, Information and Control, pp. 70–73.
8. Kannamma, A., Pavithra, K., & SubhaRani, S. (2012). Double Watermarking of DICOM Medical Images using Wavelet Decomposition Technique. *European Journal of Scientific Research*, 70, 46–55.
9. Dhanalakshmi, R., & Thaiyalnayaki, K. (2010). Dual Watermarking Scheme with Encryption. *International Journal of Computer Science and Information Security*, 7, 248–253.
10. Tripathi, S., Ramesh, N., Bernito, A., & Neeraj, K. J. (2010). A DWT based Dual Image Watermarking Technique for Authenticity and Watermark Protection. *Signal & Image Processing: An International Journal (SIPIJ)*, 1, 33–45.
11. Mahajan, L. H., & Patil, S. A. (2013). Image Watermarking Scheme using SVD. *International Journal of Advance Research in Science and Engineering*, 2, 69–77.
12. Kumar, Basant, Kumar, Shishu Bind, & Chauhan, Digvijay Singh (2014). "Wavelet Based Imperceptible Medical Image Watermarking Using Spread-Spectrum", 37th International Conference on Telecommunications and Signal Processing, Berlin Germany, 660–664, 2014.
13. Terzija, N., Repges, M., Luck, K., & Geisselhardt, W. (2002). Digital Image Watermarking Using Discrete Wavelet Transform: Performance Comparison of Error Correction Codes. International Association of Science and Technology for Development.
14. Lai, C.-C., & Tsai, C.-C. (2010). Digital Image Watermarking Using Discrete Wavelet Transform and Singular Value Decomposition. *IEEE Transactions on Instrumentation and Measurement*, 59, 3060–3063.
15. Singh, A. K., Dave, M., & Mohan, Anand (2014). Hybrid Technique for Robust and Imperceptible Dual Watermarking using Error Correcting Codes for Application in Telemedicine, Int. J. of Electronic Security and Digital Forensics, 2014 (Accepted).

16. Wu, K., Yan, W., & Du, J. (2007). "A Robust Dual Digital-Image Watermarking Technique", International conference on Computational Intelligence and security workshop, pp. 668–671.
17. Chemak, C., Bouhleb, M. S., Lapayre, J. C. (2007). "A new scheme of robust image watermarking: The double watermarking algorithm", Proceedings of the 2007 Summer Computer Simulation Conference, SCSC 2007, San Diego, California, USA, pp. 1201–1208.
18. Shen, H., & Chen, B. (2012). From Single Watermark to Dual Watermark: A New Approach for Image Watermarking. *Computer and Electrical Engineering*, 38, 1310–1324.
19. Singh, A. K., Dave, M., & Mohan, A. (2013). "Hybrid Algorithm for Image Watermarking against Signal Processing Attack", A. S. Ramanna et al. (Eds.) Proceedings of 7th Multi-Disciplinary International Workshop in Artificial Intelligence, Krabi-Thailand, Lecture Notes in Computer Science (LNCS) 8271, 235–246, 2013.
20. Singh, A. K., Dave, M., & Mohan, A. (2014). Hybrid Technique for Robust and Imperceptible Image Watermarking in DWT- DCT-SVD Domain. *National Academy Science Letters*,. doi:10.1007/s40009-014-0241-8.
21. Zinger, S., Jin, Z., & Maitre, H. (2001). Optimization of Watermarking Performances Using Error Correcting Codes and Repetition, Communications and Multimedia Security Issues of the New Century, 229–240.
22. Abdul, Wadood, Carr'e, Philippe, & Gaborit, Philippe (2013). Error correcting codes for robust color wavelet Watermarking. *EURASIP Journal on Information Security* (pp. 1–17)
23. MedPix™ Medical Image Database available at <http://rad.usuhs.mil/medpix/medpix.html>.



Amit Kumar Singh received B.Tech. in Computer Science and Engineering from Institute of Engineering and Technology, Purvanchal University Jaunpur, Uttar Pradesh in 2005. M.Tech in Computer Science and Engineering from Jaypee University of Information Technology, Wagnaghat, Solan, Himachal Pradesh in 2010. Pursuing Ph.D. from Department of Computer Engineering, NIT, Kurukshetra from 2012.



Basant Kumar working as a Assistant Professor, Department of Electronics & Comm. Engineering, Motilal Nehru National Institute of Technology, Allahabad, India



Mayank Dave working as Professor in the Department of Computer Engineering, NIT, Kurukshetra, Haryana-India. Dr. Dave obtained his Ph.D. (Computer Engineering) and M. Tech (Computer Engineering) from IIT Roorkee and he has 20 years rich experience of serving both academia and industry in various capacities.



Anand Mohan is a Professor of Electronics Engineering at Institute of Technology, Banaras Hindu University where he has held as several important administrative positions namely Member of Executive Council, Head of the Department of Electronics Engineering, Coordinator, Centre for Research in Microprocessor Applications (established by MHRD), and In charge, University Science Instrumentation Centre. Prof. Mohan has 35 years rich experience of serving both academia and industry in various capacities. *Prof. Mohan* obtained Ph.D., PG, and UG degrees in Electronics Engineering from Banaras Hindu University in 1994, 1977, and 1973 respectively. He has made notable contributions to the academic and research development in Electronics Engineering at Banaras Hindu University by creating dedicated research groups of eminent academic experts from the country and abroad. He conducted high quality research in the emerging areas like *fault tolerant / survivable system design, information security, and embedded systems*